

3D Fluid Flow and Heat Transfer Simulation of Turbulent Flow over Bank of Tubes

Motasim Shalgoum, Akram Abdullah Alharari ^a,

Talal Albireeshni, Alhosain Abdelhameed.

Mechanical Engineering Department, Faculty of Engineering, University of Zawia, Libya.

^a a.elhrari@zu.edu.ly

المخلص

يقدم هذا البحث محاكاة لتأثير عدة عوامل على أداء حزمة من الأنابيب. تم تصميم ومحاكاة تدفق ثلاثي الأبعاد مستقر لمائع مضطرب فوق حزمة من الأنابيب باستخدام برنامج (ANSYS Fluent 19.0). في هذا المشروع تم دراسة تأثير خطوات أفقية وعمودية بقيم (1.25D و 1.5D و 1.75D و 2D) وأقطار بقيم 1سم، 1.5سم، 1.75سم و 2سم على معامل انتقال الحرارة ومعامل الاحتكاك السطحي للأنابيب لتوزيع منتظم ومبعثر. وضحت النتائج أن للخطوة الأفقية والعمودية وكذلك قطر الأنبوب تأثير واضح على أداء حزمة الأنابيب لتوزيع المنتظم والمبعثر. وضحت النتائج كذلك أن الأداء الحراري للتوزيع المبعثر أفضل من المنتظم ولكن على حساب زيادة كبيرة في معامل الاحتكاك السطحي.

Abstract

This study presents a simulation of the effect of different parameters on the performance of a bank of tubes. A CFD simulation of a 3D steady state turbulent flow over a bank of tubes was designed and analyzed using ANSYS fluent 19.0. The effect of cross-wise and stream-wise pitches of 1.25D, 1.5D, 1.75D and 2D as well as diameters of 1cm, 1.5cm, 1.75cm and 2cm on the heat transfer coefficient and skin friction coefficient of the tube were studied and analyzed for both inline and staggered configurations. Results have shown that the cross-wise and stream-wise pitches and tube diameters have a noticeable effect on the performance of the tube bank for both in line and staggered configuration. Results have also shown that the staggered configuration had a better thermal performance than inline configuration.

Keywords: bank of tubes, Finite volume analysis, ANSYS, CFD simulation

Introduction

Heat exchangers are a common device used in various engineering applications to control the thermal load of a system. Most heat exchangers exchange heat between two systems via the use of fluids. Therefore, understanding the characteristics of the flow of fluids is crucial in order to enhance the thermal performance of heat exchangers. One of the most used heat exchangers in engineering applications is the "shell and tube" heat exchangers that rely on tube banks. A tube banks consist of cylindrical parallel tubes that are heated via the fluid flowing normal to it, this simulates a cross flow heat exchanger used in engineering applications and these tubes can be either staggered or in line with the flow direction [1]. Understanding the characteristics of flow tube banks is necessary in improving and optimizing the performance of heat exchangers. For any engineer, improving the performance of a system with optimum parameters is the primary point of focus of many studies. However, improving the performance of a system requires a solid understanding of the characteristics of the system as well as the parameters influencing these characteristics. To reach this level of understanding, a large amount of time and resources need to be invested in carrying out various experiments and researches. Therefore, engineers

developed multiple methods to decrease the amount of time and resources required. One of the most used methods is the use of numerical simulations that rely on well-established mathematical models and procedures such as computational fluid dynamics (CFD) [2]–[4]. Computational fluid dynamics simulation software help predict the behavior patterns and characteristics of fluid flow and heat transfer of fluid systems, such as tube banks [5]–[7]. This helps provide a general idea to the characteristics of a system as well as decreasing the required number of models and experiments that help in turn decrease the amount of time and resources invested.

For this study, a commercial CFD software ANSYS Fluent is used to analyze the thermal performance as well as the characteristics of the flow of a tube bank. This study will provide an insight to the characteristics of flow and heat transfer of a tube bank in an inline and staggered configuration as well as the effect of the Cross-wise pitch (s_t) and Stream-wise pitch (s_L) on these characteristics.

Physical model

The schematic of the model used is shown in figures 1 and 2 which represents a cross section of a shell and tube thermal heat exchanger. The front section and 3D model of the inline and staggered configuration were illustrated respectively.

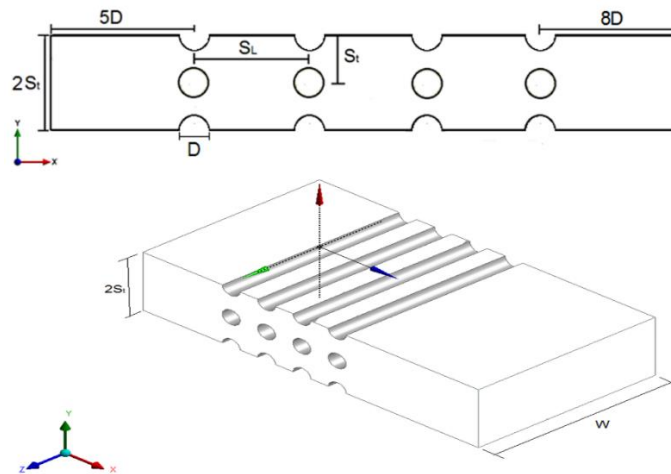


Figure 1 inline tube configuration schematic

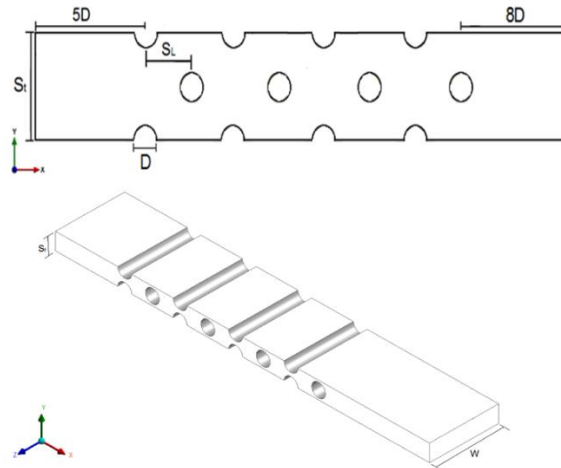


Figure 2 Staggered tube configuration schematic

Where W is the length of the tubes and width of the schematic. The Schematic dimensions include 1cm, 1.5cm, 1.75cm and 2cm tube diameters, 10cm tube length and the values of S_T and S_L that will be used for this study are 1.25D, 1.5D, 1.75D and 2D. The fluid used is air with the following material properties:

Table 1 Air material properties

	Density (ρ)(kg/m ³)	Thermal conductivity (k) (W/m ² .k)	Specific heat capacitance (cp) (j/kg.k)	Viscosity (μ) (kg/m.s)
Air	1.225	0.0242	1006.43	1.7894e-5

The most important terms in modeling a flow over bank of tubes are the tubes diameters and the cross-wise and stream-wise pitch i.e. D , S_T and S_L . both inline and staggered configurations are characterized by their cross-wise and stream-wise pitch to diameter ratio i.e.

$$a = \frac{S_T}{D} \quad (1)$$

$$b = \frac{S_L}{D} \quad (2)$$

Where a is the cross-wise pitch to diameter ratio and b is the stream-wise pitch to diameter ratio.

Assumptions

The main assumptions made when solving the problem are as follows, all walls are stationary, impermeable and no-slip conditions is valid, gravity is neglected, the flow is assumed to be turbulent and in steady state, the fluid is assumed Newtonian and incompressible with constant and homogenous material properties, and the heat transfer by radiation and viscous dissipation are neglected.

Mathematical model

The governing equations of mass, momentum, energy, turbulent kinetic energy (k) and turbulent dissipation(ϵ) are written in their general form using Cartesian coordinates based on the previously mentioned assumptions as follows [8], [9]:

- Mass (continuity) equation:

$$\frac{\partial u}{\partial x} + \frac{\partial v}{\partial y} + \frac{\partial w}{\partial z} = 0 \quad (3)$$

- Momentum equations:

$$\rho \left(u \frac{\partial u}{\partial x} + v \frac{\partial u}{\partial y} + w \frac{\partial u}{\partial z} \right) = -\frac{\partial P}{\partial x} + \mu \left(\frac{\partial^2 u}{\partial x^2} + \frac{\partial^2 u}{\partial y^2} + \frac{\partial^2 u}{\partial z^2} \right) - \frac{\partial(\overline{u'u'})}{\partial x} + \frac{\partial(\overline{u'v'})}{\partial y} + \frac{\partial(\overline{u'w'})}{\partial z} \quad (4)$$

$$\rho \left(u \frac{\partial v}{\partial x} + v \frac{\partial v}{\partial y} + w \frac{\partial v}{\partial z} \right) = -\frac{\partial P}{\partial y} + \mu \left(\frac{\partial^2 v}{\partial x^2} + \frac{\partial^2 v}{\partial y^2} + \frac{\partial^2 v}{\partial z^2} \right) - \frac{\partial(\overline{v'u'})}{\partial x} + \frac{\partial(\overline{v'v'})}{\partial y} + \frac{\partial(\overline{v'w'})}{\partial z} \quad (5)$$

$$\rho \left(u \frac{\partial w}{\partial x} + v \frac{\partial w}{\partial y} + w \frac{\partial w}{\partial z} \right) = -\frac{\partial P}{\partial z} + \mu \left(\frac{\partial^2 w}{\partial x^2} + \frac{\partial^2 w}{\partial y^2} + \frac{\partial^2 w}{\partial z^2} \right) - \frac{\partial(\overline{w'u'})}{\partial x} + \frac{\partial(\overline{w'v'})}{\partial y} + \frac{\partial(\overline{w'w'})}{\partial z} \quad (6)$$

- Energy equation:

$$u \frac{\partial T}{\partial x} + v \frac{\partial T}{\partial y} + w \frac{\partial T}{\partial z} = \alpha \left(\frac{\partial^2 T}{\partial x^2} + \frac{\partial^2 T}{\partial y^2} + \frac{\partial^2 T}{\partial z^2} \right) \quad (7)$$

- Turbulent kinetic energy (k):

$$\frac{\partial}{\partial x_i} (\rho k_t u_i) = \frac{\partial}{\partial x_j} \left[\left(\mu + \frac{\mu_t}{\sigma_k} \right) \frac{\partial k_t}{\partial x_j} \right] + P_k - \rho \epsilon \quad (8)$$

- Turbulent dissipation (ϵ):

$$\frac{\partial}{\partial x_i} (\rho \epsilon u_i) = \frac{\partial}{\partial x_j} \left[\left(\mu + \frac{\mu_t}{\sigma_\epsilon} \right) \frac{\partial \epsilon}{\partial x_j} \right] + C_1 \frac{\epsilon}{k_t} P_k - C_2 \rho \frac{\epsilon}{k_t} \quad (9)$$

Boundary Conditions

The boundary conditions used in this problem include a velocity inlet and pressure outlet for the cooling fluid and symmetrical walls at the top, bottom, front and back of the body. Figure (3) shows the boundary conditions for an inline tube distribution and figure (4) shows the boundary conditions for a staggered tube distribution.

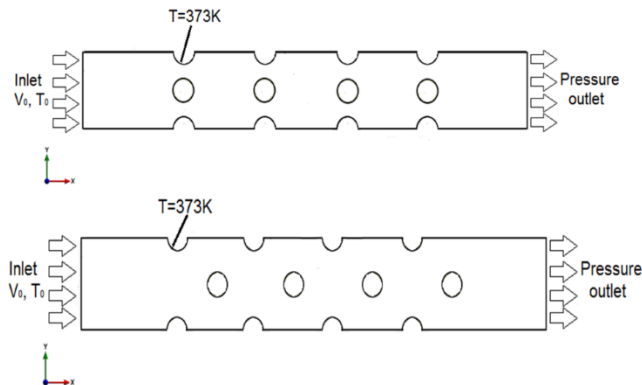


Figure 3 Inline and Staggered configuration boundary conditions

The flow of areal fluid in a tube bank body resembles that of a flow over a single cylinder with significant differences. The Reynolds number of a flow over tube bank is identified using the maximum bulk velocity U_{max} unlike a normal flow that is identified using the mean velocity U , as shown in figure (4) [10].

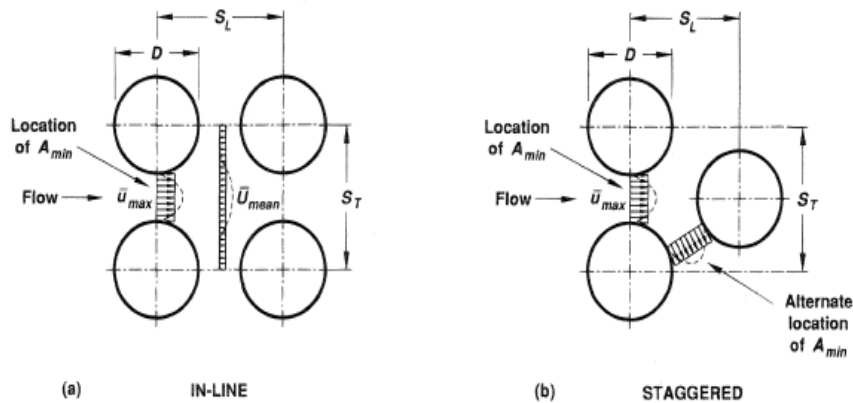


Figure 4 Schematic of a flow over a bank of tubes model for both inline (a) and staggered (b) configuration.

The Reynolds number is defined by equation (10):-

$$(10) Re = \frac{\rho \times U_{max} \times D}{\mu}$$

Where ρ is the fluids density and μ is the fluid viscosity. The maximum bulk velocity can be defined by the mean bulk velocity using equation (11) [11]–[13]:-

$$(11) \bar{U}_{max} = \frac{a}{a-1} \times \bar{U}_{mean}$$

Where U_{mean} is the mean bulk velocity. Equation (11) is used for all in-line banks, and staggered banks with $a < 2b^2 - 0.5$, for some compact staggered banks, where $a > 2b^2 - 0.5$, the minimum cross section occurs across the diagonal and therefore equation (12) becomes:-

$$\bar{U}_{max} = \frac{\sqrt{4b^2 + a - 2}}{a} \times \bar{U}_{mean} \quad (12)$$

The inlet velocities of the cooling fluid are based on Reynolds numbers in the range of 100-10000. The temperature of the tube walls are set to 373k and the cooling fluid enters the system at 300k.

Results

Mesh Dependency Study

A mesh dependency study conducted in this study compares the average heat transfer coefficient obtained from different meshes and choosing the mesh with a favorable percentage

of error. Figure (5) shows the mesh dependency study performed and figure (6) shows the final mesh used.

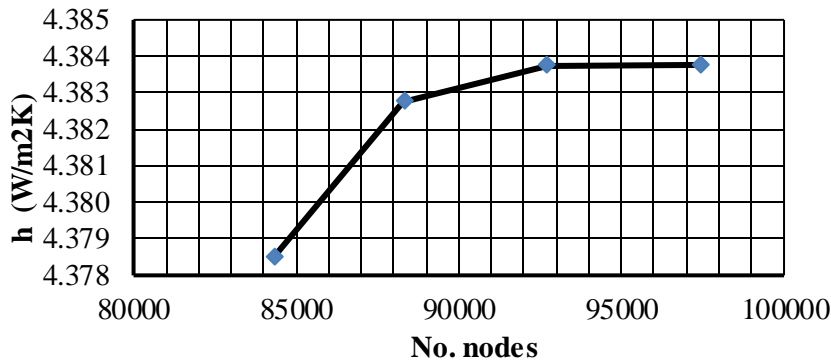


Figure 5 Mesh dependency study

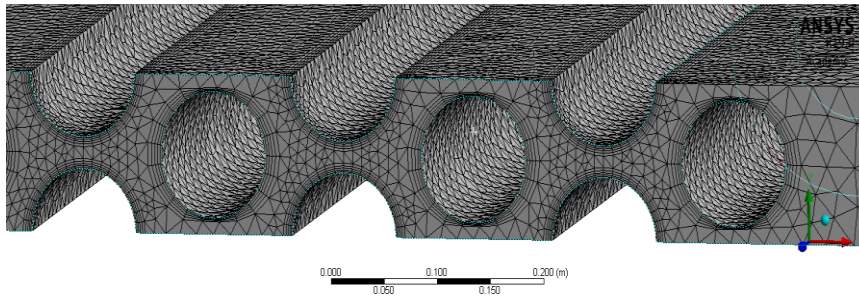


Figure 6 Example of final mesh used

As it can be seen from the previous figure, the problem was found to be mesh dependent and the mesh with 92703 nodes was chosen since it reached a desirable percentage of error (0.022%).

Model validation

In order to validate the chosen model and the results gained from it, a model validation test is performed. For this test, the results gained from the simulation are compared to results from experimental correlation. While there are many correlations that could be used, the correlation proposed by Zukauskas [12] will be used for this study. Zukauskas's correlation for an inline configuration is expressed in equation (12):-

$$Nu = 0.27 \times Re^{0.63} \times Pr^{0.36} \times \left(\frac{Pr}{Pr_s}\right)^{0.25} \quad (12)$$

Since the material properties were assumed constant, therefore Pr and Pr_s are equal, rendering equation (13) as follows:-

$$(13) Nu = 0.27 \times Re^{0.63} \times Pr^{0.36}$$

However, this equation is used for tube banks with 16 or more columns therefore a correction factor is introduced, the correlation factor used in this study is 0.86 [12]. Figure (7) show results of the model validation conducted.

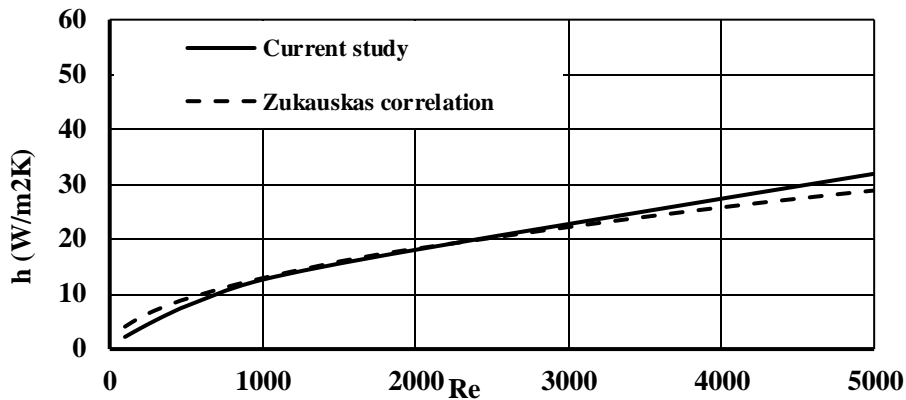


Figure 7 Comparing simulation results with experimental results

As it can be seen in the previous figure, the results gained from the simulation behaved similarly to the experimental results; however, as Reynolds number increased, these values started to deviate from the experimental results but were still within an acceptable margin of error.

Inline Configuration

Heat Transfer

Effect of cross-wise pitch

Cross-wise pitches of 1.25D, 1.5D, 1.75D and 2D will be used with a stream-wise pitch of 1.25D and tube diameter of 1cm will be used. Figure (8) illustrates the average heat transfer coefficient for all nine tubes at various cross-wise pitches.

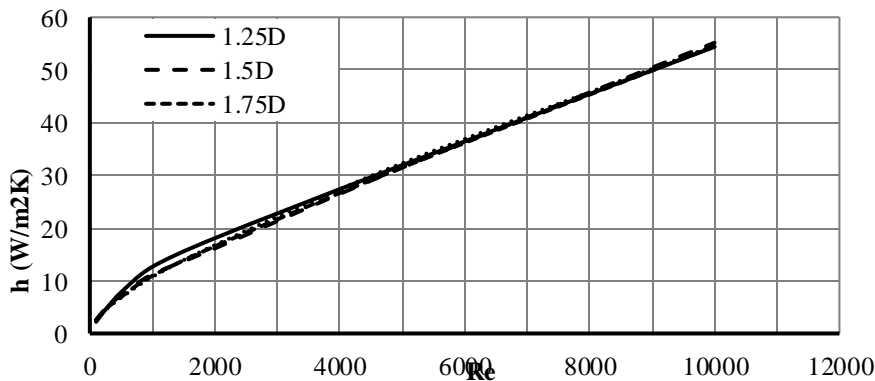


Figure 8 Average heat transfer coefficient at various Re and cross-wise pitches for $s_L=1.25D$ and $D=1\text{cm}$ (inline)

From the previous figure, increasing the cross-wise pitch led to a small decrease in heat transfer coefficient; however, as the Reynolds number increased, increasing the cross-wise pitch has had no significant impact on the heat transfer coefficient. This is probably due to each row being too far from each other to create further vortices that could increase the heat transfer coefficient and the fluid will flow in between the rows unimpeded. The previous figure also shows that an increase in Reynolds number leads to an increase in heat transfer coefficient, which is a well-established effect of increasing Reynolds number.

Effect of stream wise-pitch

As with the cross-wise pitch, stream-wise pitches of 1.25D, 1.5D, 1.75D and 2D and a diameter of 1cm will be used. As for the cross-wise pitch, a cross-wise pitch of 1.5D will be used. Figure (9) illustrates the average heat transfer coefficient for all nine tubes at various stream-wise pitches. As it can be seen from the figure, an increase in the stream-wise pitch led to an increase in the heat transfer coefficient. This is probably due to the increase in the distance between the tubes in the same row, which allows for stronger currents to develop between them. However, the effect of increasing the stream-wise pitch decreases with this increase until, eventually, it will have no more effect. Based on these results, 1.75D can be considered the optimum choice since increasing it beyond that point has no real merit in terms of heat transfer enhancement.

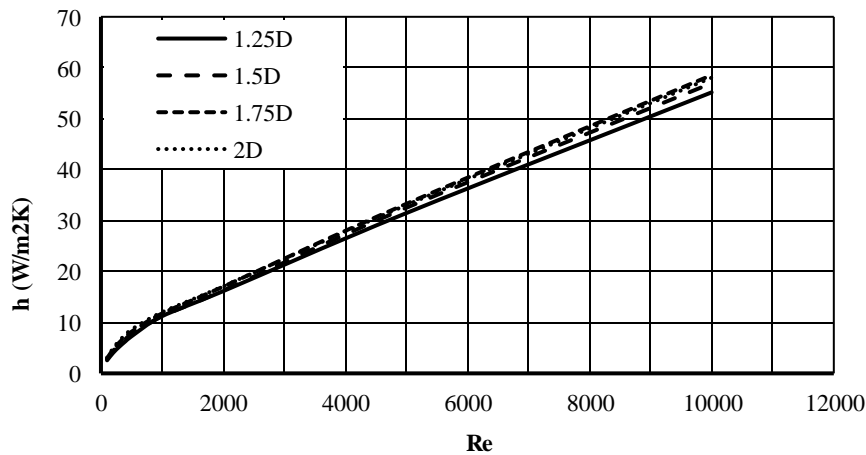


Figure 9 Average heat transfer coefficient at various Re and stream-wise pitches for $s_t=1.5D$ and $D=1\text{cm}$ (inline)

Skin Friction Coefficient

Effect of cross-wise pitch

The effect of cross-wise pitch on the skin friction coefficient is shown in figure (10). As it can be seen from the figure, an increase in cross-wise pitch leads to an increase in the skin friction coefficient. However, as the distance between tubes increases, the effect of increasing it decreases.

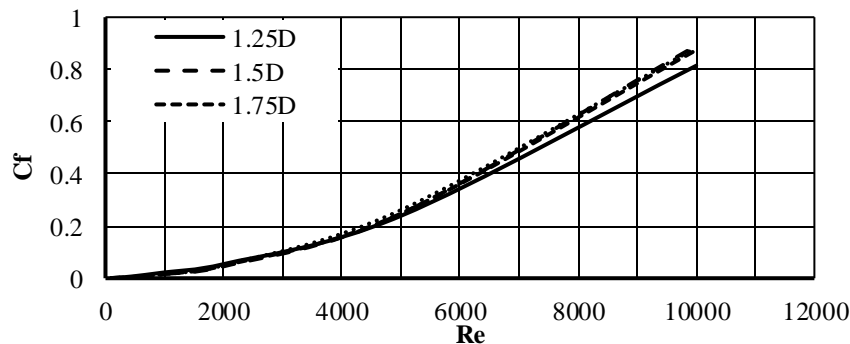


Figure 10 Average skin friction coefficient at various Reynolds numbers and cross-wise pitches for $s_L=1.25D$ and $D=1\text{cm}$ (inline)

Effect of stream-wise pitch

In order to study the effect of the stream-wise pitch, a cross-wise pitch of 1.5D and diameter of 1cm is used. Figure (11) illustrates the effect of increasing the stream-wise pitch on the skin friction coefficient.

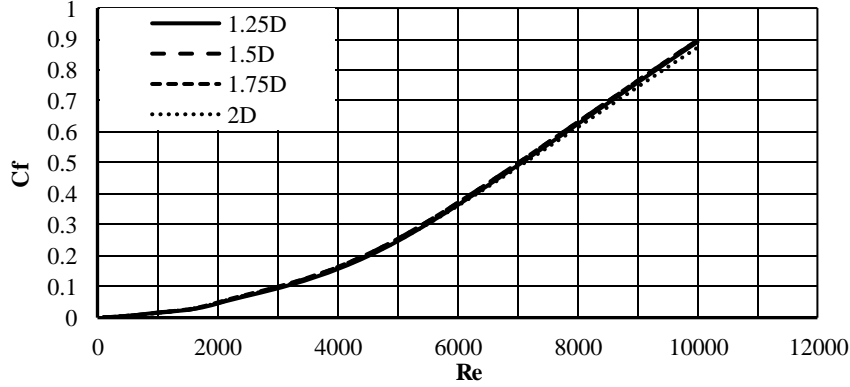


Figure 11 Average skin friction coefficient at various Reynolds numbers and stream-wise pitches for $s_t=1.5D$ and $D=1\text{cm}$ (inline)

From the previous figure, an increase in the stream-wise pitch has had a very small effect on the skin friction coefficient.

Staggered Configuration

Heat Transfer

Effect of cross-wise pitch

The effect of the cross-wise pitch on the average heat transfer coefficient for a staggered configuration at a stream-wise pitch of 1.25D is illustrated in figure (12).

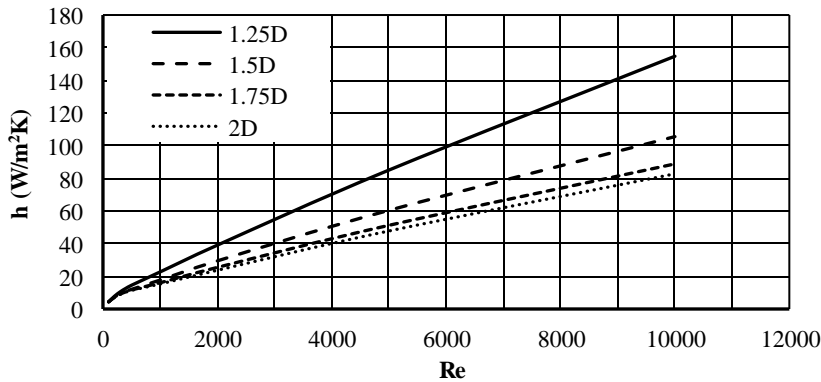


Figure 12 Average heat transfer coefficient at various Re and cross-wise pitches for $s_t=1.25D$ and $D=1\text{cm}$ (staggered)

As it can be seen from the previous figure, the increase in the cross-wise pitch has led to a decrease in the average heat transfer coefficient. This is due to the development of stronger vortices for compact staggered configurations as opposed to widely spaces configurations.

Effect of stream-wise pitch

The effect of the stream-wise pitch on the average heat transfer coefficient for a staggered configuration at a cross-wise pitch of 1.25D is illustrated in figure (13). As it can be seen from the figure, an increase in the stream-wise pitch is followed by a strong increase in the heat

transfer coefficient. This is due to the increase in the space between each column of tubes, which allow for the development of stronger currents.

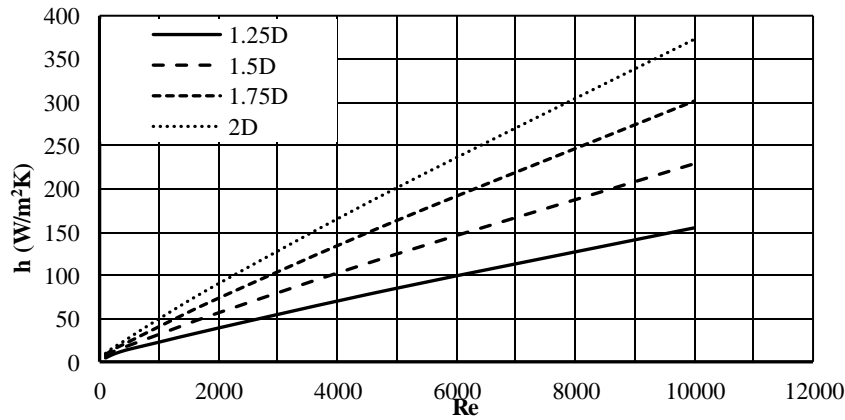


Figure 13 Average heat transfer coefficient at various Re and stream-wise pitches for $s_t=1.25D$ and $D=1\text{cm}$ (staggered)

Skin Friction Coefficient Effect of cross-wise pitch

The effect of the cross-wise pitch on the average skin friction coefficient for a staggered configuration at a stream-wise pitch of 1.25D is illustrated in figure (14). As it can be seen from the figure, increasing the cross-wise pitch decreases the skin friction coefficient.

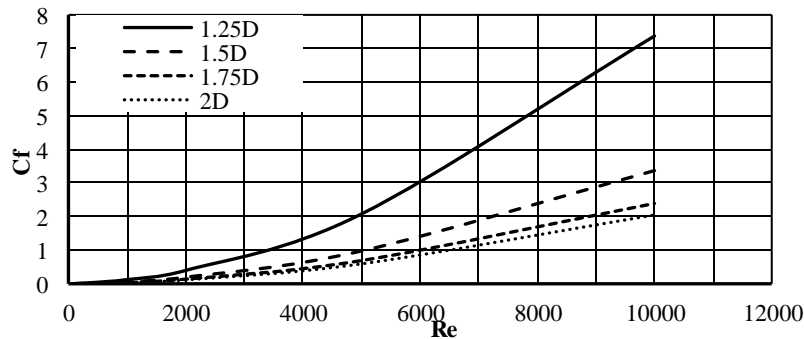


Figure 14 Average skin friction coefficient at various Reynolds numbers and cross-wise pitches for $s_t=1.25D$ and $D=1\text{cm}$ (staggered)

Effect of stream-wise pitch

The effect of the stream-wise pitch on the average skin friction coefficient for a staggered configuration at a cross-wise pitch of 1.25D is illustrated in figure (15).

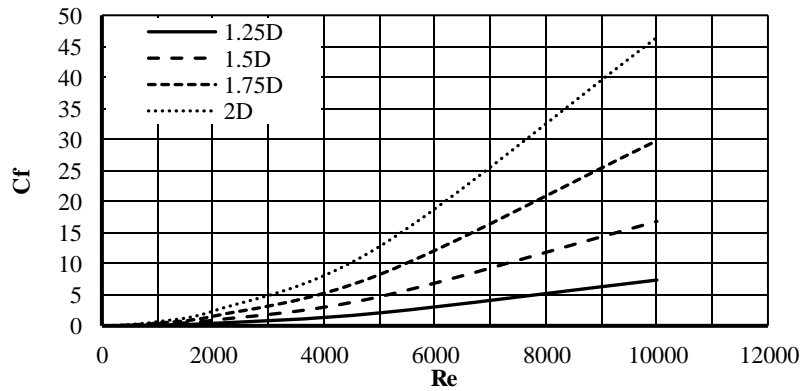


Figure 15 Average skin friction coefficient at various Reynolds numbers and stream-wise pitches for $s_t=1.25D$ and $D=1\text{cm}$ (staggered)

From the previous figure, increasing the stream-wise pitch increases the skin friction coefficient especially at higher Reynolds numbers.

Inline and staggered comparison

To compare the inline and staggered configurations to each other in order to determine the optimum configuration. For this comparison, a stream-wise and cross-wise pitch of $1.25D$ and a diameter of 1cm will be used.

Heat transfer

Results have shown that the staggered configuration had a better thermal performance when compared to an inline configuration with an average increase of 114.39% . Figure (16) illustrates this comparison between an inline and staggered configuration.

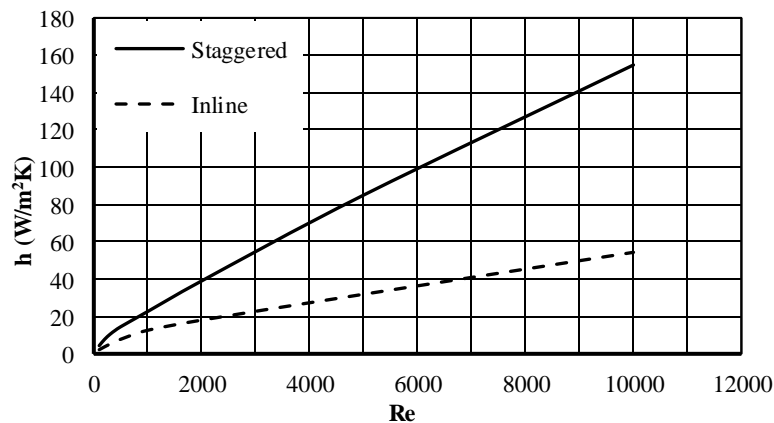


Figure 16 Average heat transfer coefficient for both staggered and inline configurations at $St=SL=1.25D$ and $D=1\text{cm}$

Skin friction coefficient

Results have shown that the staggered configuration has shown a large increase in the skin friction coefficient when compared to the inline configuration. The staggered configuration has shown an average 618.18% increase when compared to an inline configuration. Figure (17) illustrates the comparison between an inline and staggered configuration.

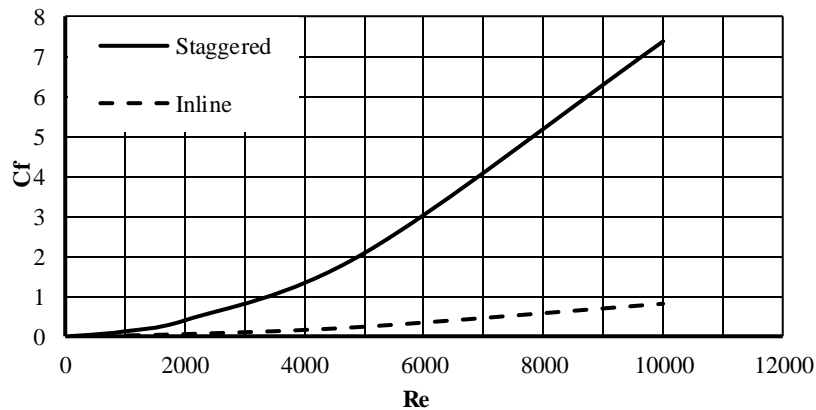


Figure 17 Average skin friction coefficient for both staggered and inline configurations at $St=SL=1.25D$ and $D=1cm$

These results show that while a staggered configuration has improved the thermal performance of the tube bank it also greatly increased the skin friction coefficient and consequently the required pressure.

Conclusion

A three-dimensional steady state model was developed to analyze and study the heat transfer and fluid flow characteristics of flow over bank of tubes. The effects of the cross-wise and stream-wise pitch on the heat transfer and flow characteristics were studied for both inline and staggered configurations. Based on the gained results, it can be concluded that the Reynolds number of the flow has a strong effect on the performance of tube banks. The cross-wise and steam-wise pitches has a strong effect on the performance of the tube bank especially in the staggered configuration. The staggered configuration has shown a better thermal performance than the inline configuration, however at a cost of a greatly increased pressure drop, as evident by the high friction factor.

References

- [1]I. Ikpotokin and C. O. Osueke, "Heat Transfer and Fluid Flow Characteristics Study for In-Line Tube Bank in Cross-Flow," *Int. J. Mech. Mechatronics Eng.*, vol. 14, no. 03, p. 13, 2014.
- [2]M. S. Kamel and S. M. Najm, "Heat transfer and fluid flow over a bank of circular tubes heat exchanger using nanofluids: CFD simulation," *IOP Conf. Ser. Mater. Sci. Eng.*, vol. 928, no. 2, 2020, doi: 10.1088/1757-899X/928/2/022017.
- [3]P. D Souza, D. Biswas, and S. P. Deshmukh, "Air side performance of tube bank of an evaporator in a window air-conditioner by CFD simulation with different circular tubes with uniform transverse pitch variation," *Int. J. Thermofluids*, vol. 3–4, 2020, doi: 10.1016/j.ijft.2020.100028.
- [4]H. Iacovides, B. Launder, and A. West, "A comparison and assessment of approaches for modelling flow over in-line tube banks," *Int. J. Heat Fluid Flow*, vol. 49, no. C, pp. 69–79, 2014, doi: 10.1016/j.ijheatfluidflow.2014.05.011.
- [5]D. V. Nagappan *et al.*, "CFD Analysis of Heat Exchanger Over a Staggered Tube Bank for Different Angle Arrangement of Tube Banks," *J. Des. Sustain. Environ.*, vol. 5, no. 2, pp. 18–22, 2023.
- [6]S. Li and X. Zhao, "Experimental Study and Cfd Simulation of Heat Transfer and Friction

- Factor Characteristics in the Crossflow Tube Bank,” *Comput. Therm. Sci.*, vol. 14, no. 5, pp. 21–46, 2022, doi: 10.1615/ComputThermalScien.2022042368.
- [7] J. Xu, J. Li, Y. Ding, Q. Fu, M. Cheng, and Q. Liao, “Numerical simulation of the flow and heat-transfer characteristics of an aligned external three-dimensional rectangular-finned tube bank,” *Appl. Therm. Eng.*, vol. 145, pp. 110–122, 2018, doi: 10.1016/j.applthermaleng.2018.09.022.
- [8] J. Anderson, *Computational Fluid Dynamics: The Basis with Applications*. 1995.
- [9] A. M. Vaidya, N. K. Maheshwari, and P. K. Vijayan, “Development of a Cartesian grid based CFD solver (CARBS).” 2013.
- [10] F. Balleari, “CFD characterization of a liquid jets heat exchanger,” University of Genoa, 2021.
- [11] O. P. Bergelin, M. D. Leighton, W. L. J. Lafferty, and R. L. Pigford, *Heat transfer and pressure drop during viscous and turbulent flow across baffled and unbaffled tube banks*. Newark, Del., 1958.
- [12] A. Žukauskas and R. Ulinskas, “Efficiency parameters for heat transfer in tube banks,” *Heat Transf. Eng.*, vol. 6, no. 1, pp. 19–25, 1985, doi: 10.1080/01457638508939614.
- [13] ESDU, “Convective heat transfer during crossflow of fluids over plain tube banks.,” *ESDU Int. Plc*, vol. 73031, no. November, 1973.